energies

MDPI

Article

Analysis of the Performance of a Passive Downdraught Evaporative Cooling System Driven by Solar Chimneys in a Residential Building by Using an Experimentally Validated TRNSYS Model

Andrés Soto [1,*], Pedro Martínez [1], Victor M. Soto [2] and Pedro J. Martínez [1]

[1] Department of Mechanical Engineering and Energy, Miguel Hernández University, Avda. Universidad, s/n, Ed. Innova, 03202 Elche, Spain; pedro.martinez@umh.es (P.M.); pjuan.martinez@umh.es (P.J.M.)
[2] Department of Applied Thermodynamics, Polytechnic University of Valencia, Camino de Vera, s/n, 46022 Valencia, Spain; vsoto@ter.upv.es
* Correspondence: andres.sotob@coiirm.es

Abstract: Natural ventilation, combined with a passive cooling system, can provide significant energy savings in the refrigeration of indoor spaces. The performance of these systems is highly dependent on outdoor climatic conditions. The objective of this study was to analyse the feasibility of a passive, downdraught, evaporative cooling system driven by solar chimneys in different climatic zones by using an experimentally validated simulation tool. This tool combined a ventilation model and a thermal model of the dwelling in which an empirical model of a direct evaporative system made of plastic mesh was implemented. For experimental validation of the combined model, sensors were installed in the dwelling and calibrated in the laboratory. The combined model was applied to Spanish and European cities with different climates. In the simulation, values of cooling energy per volume of air ranging between 0.53 Wh/m^3 and 0.79 Wh/m^3 were obtained for Alicante (hot climate with moderate humidity) and Madrid (hot and dry climate), respectively. In these locations, medium and high applicability was obtained, respectively, in comparison with Burgos (cold climate with moderate humidity) and Bilbao (cold and humid climate), which were low. The evaluation of the reference building in each location allowed establishing a classification in terms of performance, comfort and applicability for each climate.

Keywords: evaporative cooling; wind tower; solar chimneys; solar cooling; TRNSYS simulation

Citation: Soto, A.; Martínez, P.; Soto, V.M.; Martínez, P.J. Analysis of the Performance of a Passive Downdraught Evaporative Cooling System Driven by Solar Chimneys in a Residential Building by Using an Experimentally Validated TRNSYS Model. *Energies* **2021**, *14*, 3486. https://doi.org/10.3390/en14123486

Academic Editor: Carlo Renno

Received: 4 May 2021
Accepted: 9 June 2021
Published: 11 June 2021

1. Introduction

Information from the European Commission states that HVAC systems are responsible for 50% of the energy consumed in buildings. Directive (EU) 2018/844 which amended Directive 2010/31/EU, sets a target of 80–95% reduction of greenhouse gas emissions in buildings by the year 2050 compared to 1990. In this context, the concept of nearly zero energy consumption (nZEB) involves the use of energy efficiency to reduce energy demand to a minimum as well as the use of renewable energies.

The use of natural ventilation strategies contributes to the reduction of cooling energy demand during periods when outdoor conditions are able to provide indoor comfort. However, in the summer months, this situation is difficult to achieve on days when the outside temperature is high and additional cooling sources are required.

Solar radiation can be used to produce passive ventilation and cooling in buildings through elements that utilise and transform the energy produced by the sun in order to take advantage of it for cooling strategies. According to Monghasemi and Vadiee [1], solar chimneys can be integrated into solutions for space heating and cooling. The air contained

in the chimney is heated when a surface with high energy collection is exposed to solar radiation that transfers it into the chimney cavity. The temperature difference of the air in the chimney and the room causes an extraction operation due to the buoyancy effect. In [2], optimum air flow rates were obtained for a 45°angle of inclination of the surface that received the radiation.

Evaporative cooling, combined with natural ventilation, has the potential to reduce outdoor air temperatures in hot climates with moderate humidity by harnessing the latent heat of water in an adiabatic process. Evaporative cooling systems can be used for temperature control of both outdoor and indoor spaces. Givoni, B. developed an evaporative cooling system to cool the outdoor areas of the Expo '92 in Seville. This system consisted of a duct that caught outside air at the top and sprayed water controlled by a pump. The passive downdraught evaporative cooling (PDEC) system cools the air at the top of the building to produce an airflow down to the lower spaces [3]. Cuce et al. [4] presented other designs that could be combined with wind towers such as using an evaporative cooling pad at the intake of outdoor air. The temperature reduction provided by PDEC systems, according to the research reviewed in [5], can be as much as 8 °C for outdoor ambient temperatures above 35 °C.

There are different materials that can be appropriate for the manufacture of the pad used as a direct evaporative system: porous metal pads, cellulose pads, porous ceramic pads and plastic polymer pads. Rong et al. [6] studied the performance of a cellulose pad under different modes of control and operation. The highest temperature drop was obtained when the inlet air velocity increased to its highest value. When the water supply to the pad was increased, the pressure drop increased as well. Other authors [7] developed a numerical model for an aluminium, multilayer pad (Oxyvap cooler). In [8], the optimisation of a cellulose pad, based on the multi-objective method to improve thermodynamic and life cycle performance, was presented. They obtained optimal pad thicknesses for most cases between 0.23 and 0.24 m and a contact area of 540 m^2/m^3. Experimental results of a new pad design with beehive construction, made of corrugated cellulose were presented in [9], wherein 84% efficiency was obtained. New natural materials were presented and compared in [10]. The highest water consumption was obtained for pads made of eucalyptus fibres. In this study, higher evaporation rates were obtained for all materials when the air velocity was higher. The different parameters affecting the design of an evaporative pad were evaluated in different climates in Morocco [11]. In all cases, the cooling capacity (mass flow rate of cooled air) was found to increase for higher thicknesses and increasing frontal air velocity. However, the performance (saturation effectiveness) was lower for lower thicknesses and increasing air velocity. Water consumption ranged between 3.3 kg/h and 10.6 kg/h. Similar conclusions were obtained in [12] for different climatic zones of Iran. The performance of the evaporative pad could be increased by predrying the intake air with desiccants or membranes [13]. A new arrangement for an evaporative pad consisting of a multi-layer section was proposed in [14].

The application potential of evaporative cooling systems has a strong dependence on the local climate. Aparicio-Ruiz et al. [15] studied the potential of applying a PDEC system in different climates in the USA by establishing a set of maps derived from evaluating two proposed indexes based on US meteorological databases. Other authors [16,17] proposed an index for the calculation of climatic cooling potential and energy savings through evaluation using climatic data from different zones of the Iberian Peninsula.

Kang et al. [18] obtained a mathematical correlation for spray PDEC systems that accurately predicted the temperature, humidity and velocity of the air flowing out of the systems. These authors developed in [19] a CFD model that enabled predicting the airflow characteristics in PDEC systems and the relationship with system performance under different humidity conditions. They concluded that PDEC systems had a strong dependence on the local climate.

The aim of the study is to simulate a solar chimney-driven PDEC system in different proposed climate zones in order to evaluate performance and applicability, defined as the

quality of the evaporative system for application in a specific climate. An empirical model of a novel, direct-evaporative cooling pad made of plastic mesh was used as the cooling solution for the intake air to the PDEC system. This panel was characterised by its low manufacturing cost; being configurable in many sizes, flexible and adaptable; and furthermore, the resulting air pressure drop was low. Both the empirical model of the evaporative pad as well as the ventilation and thermal model of the house were experimentally validated and implemented together in a building energy model. The model integrated the building envelope flow model, which incorporated the passive ventilation solutions (PDEC and solar chimneys) with the multi-zone thermal model. The performance of the proposed system was therefore evaluated in a specific reference building, through an energy model, in different climatic zones. The study of the performance and comfort values obtained by each system under different climatic conditions and configurations allowed us to define a suitable selection for each climate zone in terms of technology type and configuration. This is a novelty for the integration of this solution in future projects and the fulfilment of the objectives established by the EU.

2. Materials and Methods

The building energy simulation that incorporated the passive cooling system described below was based on the integration of two experimentally validated models. The combined ventilation and thermal model of the house integrated the calculation of flow rates through the building envelope and the prediction of indoor temperatures in each zone. This model was experimentally validated using on-site collected data that included the measurement of air velocities through openings, indoor comfort conditions and outdoor weather conditions. This validation was complemented with a laboratory test for the calibration of the couplings where the air velocity probes (hot-wire probes) were placed, which allowed the relationship between the measured air velocity and the air flow through the couplings to be obtained. The mathematical model of the evaporative system included the mathematical equations that predicted the air temperature at the outlet of the system and the pressure drop. To obtain the experimental data, a wind tunnel was used and equipped with a water supply, collection and recirculation system with an adjustable flow rate. The thermal- and fluid-dynamic behaviour of the C&V RF-200 model evaporative pad provided by Control and Ventilation S.L. was characterised for different thicknesses, airflows and incoming water flow rates, and a non-linear regression analysis was conducted for the constant terms calculation.

This ventilation model has certain limitations. The wind speed and indoor temperatures were considered constant for every time step (1 h) of the simulation. Temperatures were considered to be uniform across the zones and with vertical variation in the solar chimneys. Flow field on the building envelope was considered using a correlation for the pressure coefficients around the building (function of the geometric parameters of the building and the wind direction angle).

2.1. Building and Evaporative Cooling System Description

The reference house (Figure 1a), located in Murcia (Spain), incorporated a natural ventilation system consisting of a north-facing wind tower (Figure 1b) assisted by four solar chimneys that communicated with the rooms of the building (Figure 1c). The wind tower favoured the natural inflow of outside air by producing a downward flow caused by the air velocity and pressure of the wind as it impinged on the façade openings. The air flow through the spaces was produced by convective ventilation wherein the air was extracted by the buoyancy effects and temperature differences that occurred in the chimneys. The solar chimneys had different geometries and were 2 m high. The solar radiation absorption surface consisted of a sheet of iron painted black.

Figure 1. (**a**) Reference building; (**b**) Wind tower; (**c**) Building distribution.

In combination with the natural ventilation system described above, the house had a high thermal inertia. The walls acted as an energy store during the day. At night, ventilation was increased by the effect of the temperature difference, and this energy was dissipated when the outdoor temperature was lower than the indoor temperature.

The dwelling exhibited several ventilation modes, which depended on the outdoor conditions and the strategy considered. These ventilation modes were simulated and experimentally validated in a previous study [20]. For this experimental validation, a hot-wire probe (Testo 440) was placed in the centre of the inlet section of each solar chimney to determine the temperature and air velocity. In the living room, the most occupied space, a Testo 480 multi-function instrument was installed to measure indoor air quality (IAQ) parameters and the predicted percentage of dissatisfied (PPD). The PPD index provides a quantitative prediction of the number of people who will be dissatisfied with the level of thermal comfort inside the house. This value was calculated directly according to ISO 7730, by the software integrated into the instrument, as a function of the measured indoor air and radiation temperatures, air velocity and relative humidity. The weather station (PCE-FWS 20N) was placed at the top of the building, and the electrical energy consumption was measured with a Circutor Myebox 1500 analyser. For the calibration test of the couplings, a Testo 420 balometer was used.

The evaporative system considered in the simulation consisted of a grid or mesh made of polyethylene wire with a diameter of 0.7 mm and measurements of 4 × 4 mm, according to the UNE-62.001 standard. The resulting compactness was 117.2 m^2/m^3, and it was characterised by good efficiency, low pressure drop and low installation and maintenance costs. The minimum water flow rate for the evaporative pad recommended by the manufacturer was 20 l/min of water per square metre of exposed horizontal (upper) surface of the pad.

In the empirical test presented in [21], a pad with dimensions 492 × 712 mm was characterised for thicknesses of 80, 160 and 250 mm. A total of 91 tests were conducted for different airflows and water flow rates.

2.2. Model Description

The simulation of the PDEC system driven by solar chimneys was conducted using the building energy model developed from the experimentally validated models presented in [20,21].

The inlet air was led through a direct evaporative pad and introduced into the tower that distributed the cooler air to the different zones of the house, according to the scheme in Figures 2 and 3. The air inside was driven by forces that favoured its movement: wind pressure at the opening, suction at the solar chimneys and lower temperature at the tower that generated a downdraft of air.

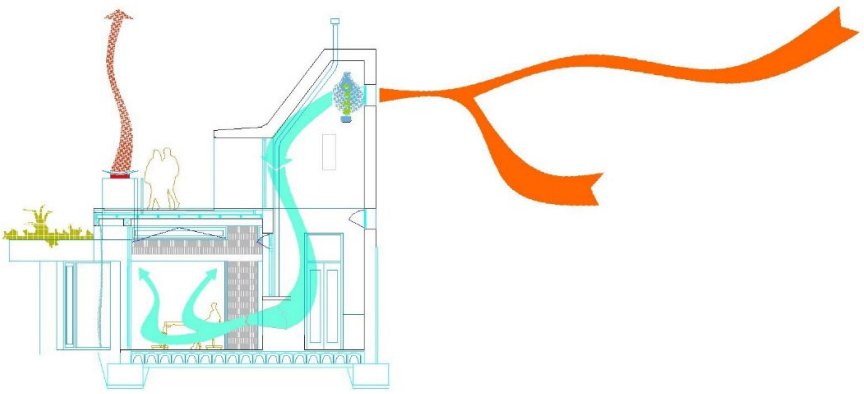

Figure 2. Cooling system (PDEC) proposed.

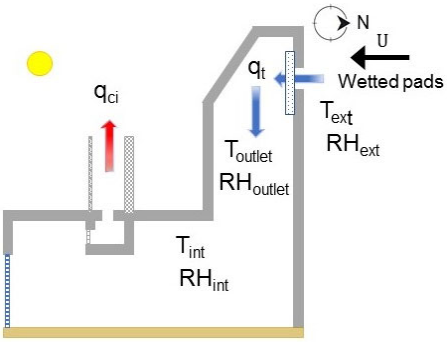

Figure 3. PDEC operating diagram.

The energy model was conducted in TRNSYS (Transient System Simulation Tool) [22] and included the combination of the envelope ventilation flow model developed in EES (Engineering Equation Solver) [23] and the multi-zone thermal model. A solution was obtained for the ventilation flow rates and temperatures for each zone. TRNSYS is a building energy simulation program for dynamic processes that, through its calculation engine, can be connected to other non-linear equation solving tools such as EES through functions called "types". EES has a large database of thermodynamic functions and variables that allow the development of complex energy models.

The mathematical equations, coefficients and correlations that make up the mathematical model described are presented below.

The movement of air within spaces and through openings is driven by pressure differences, according to Bernoulli's principle. The Conservation of Mass principle states that the sum of the mass flow rate of air through the building envelope is equal to zero.

The calculation of the flow rate (q_i) at each opening is obtained from Equation (1) from the pressure differential (Δp_i) and the effective area (A_i).

$$q_i = Cd_i \cdot A_i \cdot M_i \sqrt{\frac{2 \cdot |\Delta p_i|}{\rho_E}} \quad (1)$$

where "*M*" is the sign of the pressure differential; *M* = +1 for the flow entering the space, and *M* = −1 for the flow leaving the space.

The pressure differential at the inlet of the downdraft evaporative system and at the outlet of the chimney is represented by the diagram shown in Figure 4 and given by the following expressions, respectively:#

$$\Delta p_i = \Delta p_0 - \rho_E \cdot g \cdot z_i + \rho_I \cdot g \cdot z_i + \frac{1}{2} \cdot \rho_E \cdot U^2 \cdot Cp_i - \Delta p_{eva} \quad (2)$$

$$\Delta p_{ci} = \Delta p_0 - \rho_E \cdot g \cdot z_{ci} + \rho_I \cdot g \cdot H + \rho_{ci} \cdot g \cdot L \quad (3)$$

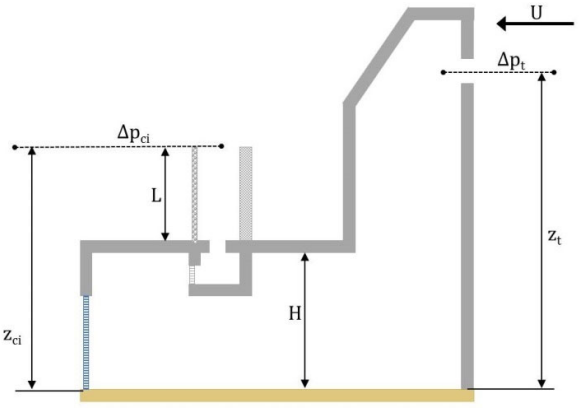

Figure 4. Pressure differentials.

The principle of conservation of mass of the system was defined by the following expression:

$$\sum \rho_i \cdot q_i = 0 \quad (4)$$

The discharge coefficient at the outlet section of the chimney was calculated using Equations (5) and (6), which considered the sections of the chimney which the air passed through: the absorption grid, inlet tube to the cavity and outlet section of the chimney.

$$\frac{1}{A_{ci\,eff}^2} = \frac{1}{(Cd_{ci} \cdot A_{ci\,out})^2} = \sum \frac{1}{(Cd_{ci\,section} \cdot A_{ci\,section})^2} \quad (5)$$

$$Cd_{ci} = \frac{1}{A_{ci\,out} \cdot \sqrt{\sum \frac{1}{(Cd_{ci\,section} \cdot A_{ci\,section})^2}}} = \frac{1}{A_{ci\,out} \cdot \sqrt{\frac{1}{(Cd_{ci\,out} \cdot A_{ci\,out})^2} + \frac{1}{(Cd_{ci\,in} \cdot A_{ci\,in})^2} + \frac{1}{(Cd_{ci\,grid} \cdot A_{ci\,grid})^2}}} \quad (6)$$

$A_{t\ eff} = Cd_t A_t$ is the effective area of the opening, $Cd_{ci\ out}$ and $A_{ci\ out}$ are the discharge coefficient and the area of the chimney at the outlet and $Cd_{ci\ in}$ and $A_{ci\ in}$ at the inlet. $Cd_{ci\ grid}$ and $A_{ci\ grid}$ are the discharge coefficient and the area on the absorption grid, respectively (Figure 5a). The inlet section corresponded to a 160 mm diameter tube. Chimney 1 was composed of two tubes, while the other chimneys had only one tube. Chimney 2 did not have an absorption grid.

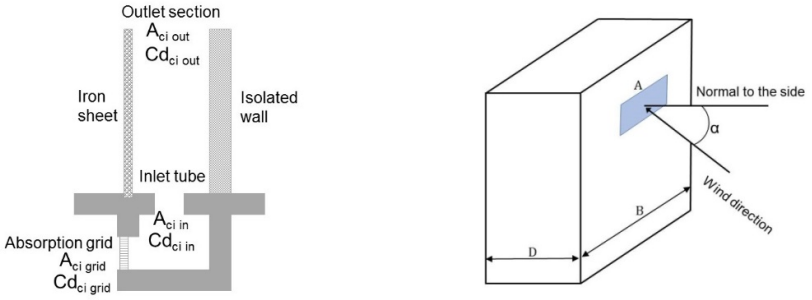

Figure 5. (**a**) Solar chimney discharge coefficient; (**b**) Pressure coefficient parameters.

The wind pressure coefficient at the air inlet opening was obtained using the correlation of Muehleisen and Patrizi [24] for a low-rise building:

$$Cp_t = \frac{16.12\cdot10^{-1}-1.78\cdot10^{-1}\cdot G-1.15\cdot10^{-2}\cdot\alpha+3.28\cdot10^{-5}\cdot\alpha^2+1.67\cdot10^{-3}\cdot G\cdot\alpha}{1-3.12\cdot10^{-1}\cdot G-1.59\cdot10^{-2}\cdot\alpha+9.82\cdot10^{-5}\cdot\alpha^2+2.15\cdot10^{-3}\cdot G\cdot\alpha} \quad (7)$$

where α is the angle between the normal to the side under consideration and the wind direction, S = D/B is the ratio depth to the breadth from the side under consideration and G = ln(S).

The efficiency of the evaporative cooling system can be expressed according to Equation (8), where T_{eva} is the temperature at the outlet of the evaporative system, T_{wb} the wet bulb temperature and T_E the outside temperature.

$$\eta = \frac{(T_E - T_{eva})}{(T_E - T_{wb})} \quad (8)$$

As presented in [21], the efficiency (η) and pressure drop (Δp_{eva}) in the evaporative pad can be modelled using the empirical correlations below as a function of air velocity and inlet air flow rate (v_t y q_t), pad thickness (l), water recirculation flow rate (q_{rw}) and the introduction of the geometrical non-dimensional parameter (l/le):

$$\eta = 1 - \exp\left(-\frac{\beta_2 \cdot l^m}{v_t^n}\right) \quad (9)$$

$$\Delta p_{eva} = d_2 \cdot \left(\frac{l_e}{l}\right)^{e_2} \cdot \left(1 + f_2 \cdot \frac{q_{rw}}{q_t}\right) \cdot \frac{\rho_E \cdot {v_t}^2}{2} \quad (10)$$

2.3. TRNSYS Modelling

The mathematical model presented in the previous section was implemented in the EES environment. The output variables of this model (flow rates) were called input variables by the thermal model of the building in TRNSYS, according to the methodology presented in [20], to calculate the indoor temperatures of each zone as output variables. The two models iterated at each time step until they converged to a solution for both variables (flow rates and indoor temperatures).

The energy model developed in TRNSYS, which combined the mathematical model implemented in EES and the multi-zone thermal model, is shown in Figure 6.

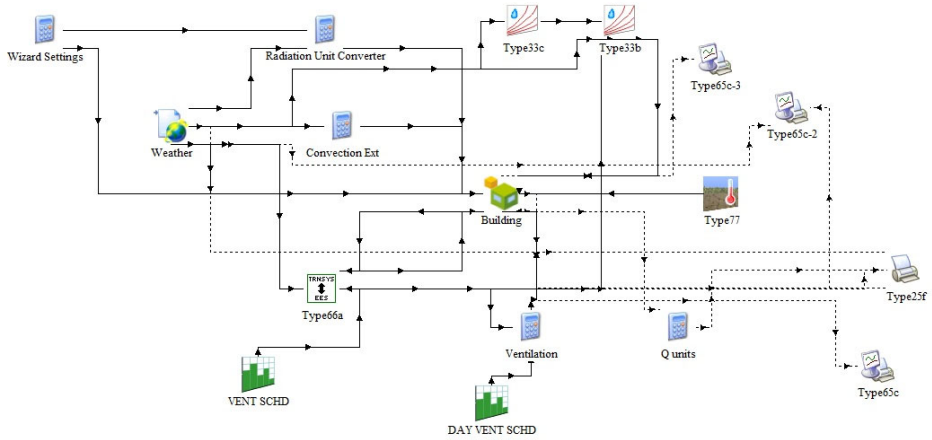

Figure 6. Model simulation in TRNSYS.

The iteration scheme of both models is depicted in Figure 7a. The results of the flow rates calculated by the envelope model developed in ESS were called through function type 66a and introduced into the building thermal model in TRNSYS (type 56) to obtain the temperatures of each zone. These values were returned as inputs to the ventilation envelope model. Figure 7b shows the inputs and outputs of the ventilation and thermal models.

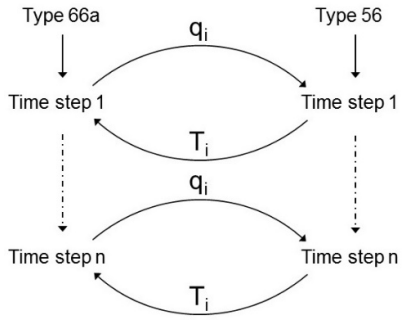

(**a**)

Envelope (type66a)			Thermal multi-zone (type56)		
	Inputs	Description		Inputs	Description
Outputs type56	T_{lr}	Living room air temp.	Outputs type66a	q_{c1}	Vol. airflow chimney 1
	T_{lt}	Tower air temp.		q_{c2}	Vol. airflow chimney 2
	T_{lr1}	Bedroom 1 air temp.		q_{c3}	Vol. airflow chimney 3
	T_{lr3}	Bedroom 3 air temp.		q_{c4}	Vol. airflow chimney 4
	T_{c1}	Chimney 1 air temp.		m_{c1}	Mass airflow chimney 1
	T_{c2}	Chimney 2 air temp.		m_{c2}	Mass airflow chimney 2
	T_{c3}	Chimney 3 air temp.		m_{c3}	Mass airflow chimney 3
	T_{c4}	Chimney 2 air temp.		m_{c4}	Mass airflow chimney 1
Outputs type15	T_E	Outdoor temp.	Outputs type15	T_E	Outdoor temp.
	U	Wind velocity		T_{SKY}	Sky temp.
	alpha	Wind direction		T_{GROUND}	Ground temp.

(**b**)

Figure 7. (**a**) Iteration method; (**b**) Inputs and outputs.

The evaporative outlet temperature was calculated from the pad efficiency, according to Equation (9). To obtain the outlet relative humidity, the cooling evaporation process was considered isenthalpic. The model was capable of predicting consistent results for indoor temperature and flow rate, provided by the PDEC system at each time base (1 h).

3. Results

The described PDEC system was evaluated in the reference building, using the meteonorm [25] climatic database of a typical year for the locations shown in Figure 8 (Alicante, Bilbao, Burgos, Lisbon, Madrid, Malaga and Rome). The simulation was conducted for the period of July and August (1488 h).

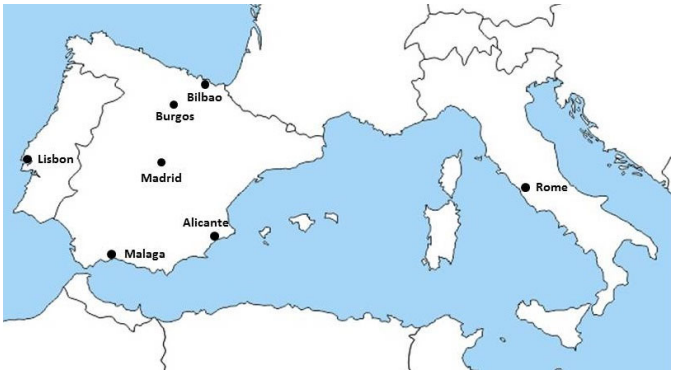

Figure 8. Climatic locations.

3.1. Weather Analysis

As can be seen in Figure 9, the evolution of the outdoor temperature during the period analysed showed differences at each site. The predominant difference was 8 °C between the coldest and the hottest climate. This difference was reduced to 4 °C in the second and fourth week of July and the third week of August. In the second week of August, this differential reached 10 °C. The disparity in weather conditions between the different climates resulted in different performances of the PDEC system. The average values of the outdoor conditions for each location in the analysed period are shown in Table 1. The psychometric diagrams are shown in Figure 10. Five climate types are established according to these parameters:

- Climate 1: hot and dry, T_E >25 °C, RH < 40% (Madrid);
- Climate 2: hot and moderate humidity, T_E > 25 °C, 40% < RH < 65% (Alicante, Málaga);
- Climate 3: cold and moderate humidity, T_E < 21 °C, 40% < RH < 65% (Burgos);
- Climate 4: cold and wet, T_E < 21 °C, RH > 65% (Bilbao);
- Climate 5: temperate and wet, 21 °C < T_E < 25 °C, RH > 65% (Lisbon, Rome).

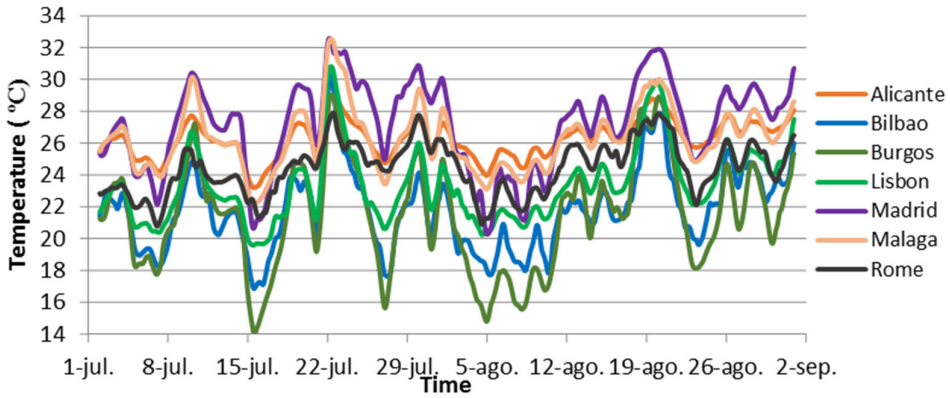

Figure 9. Average daily outdoor temperature.

Table 1. Meteorological data.

Location	T_E (°C)	RH (%)	T_{wb} (°C)	R horiz. W/m²	U (m/s)	Alpha (°)
Alicante	26	61	17.5	523	2	20
Bilbao	21	69.5	15	350.5	2	270
Burgos	21	53	10	495.5	4	5
Lisbon	22	65	14	505.5	5	345
Madrid	26.5	32.5	8	500.5	2	5
Málaga	26	55	15.5	516	2	70
Rome	23	72.5	17.5	397	3	200

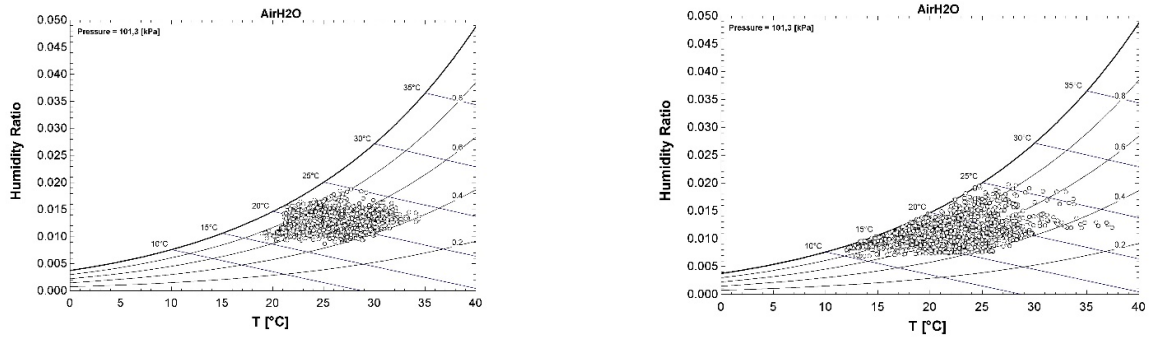

(**a**) (**b**)

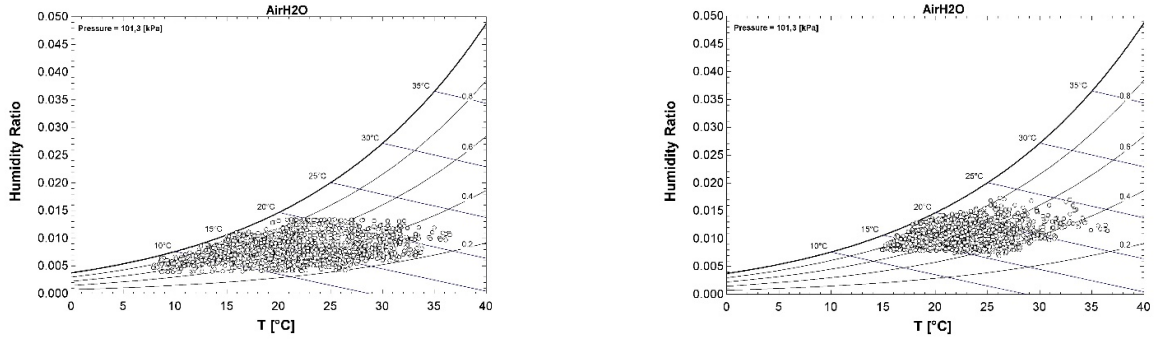

(**c**) (**d**)

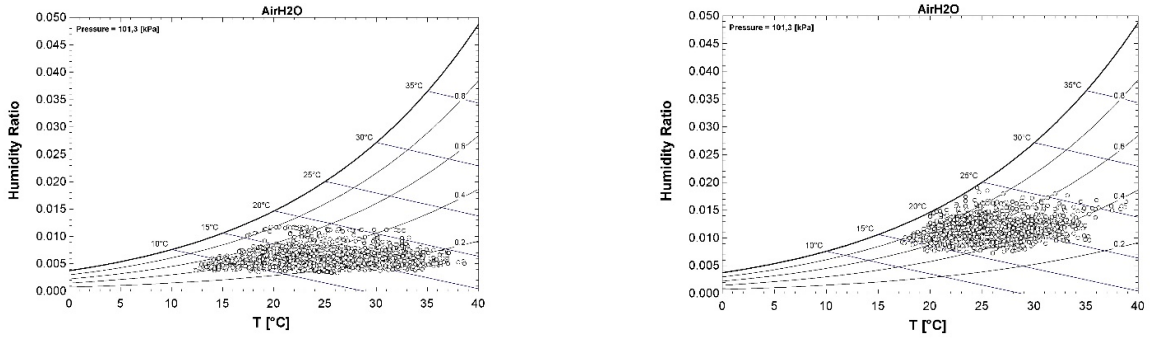

(**e**) (**f**)

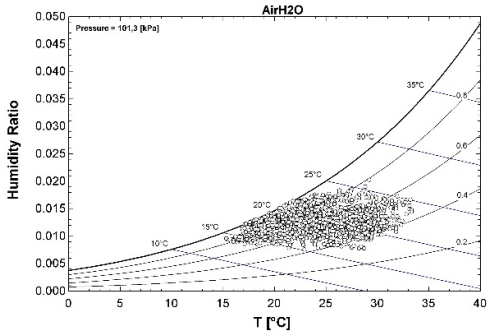

(**g**)ǂ

Figure 10. Summer climatic conditions for (**a**) Alicante (SCV1); (**b**) Bilbao (SCV2); (**c**) Burgos (SCV3); (**d**) Lisbon (SCV4); (**e**) Madrid (SCV5); (**f**) Málaga (SCV6); (**g**) Rome (SCV7).

3.2. Simulation Analysis

The input data and the values resulting from the calibration and parametric fit of the model in TRNSYS were presented in [20]. The results are shown in Table 2.

Table 2. Inputs for airflow envelope model.

Input	Chim 1	Chim 2	Chim 3	Chim 4	Tower
H (m) room height	2.5	2.5	2.5	2.5	-
L (m) chimney height	2	2	2	2	-
z (m) height of opening above ground level	4.5	4.5	4.5	4.5	4.65
A_{out} (m^2) outlet area	0.323	0.056	0.296	0.22	0.95
A_{in} (m^2) inlet area	0.040	0.020	0.020	0.020	-
A_{grid} (m^2) grid area	0.057	-	0.057	0.057	-
Cd_{out} outlet discharged coefficient	0.6	0.6	0.6	0.6	0.4
Cd_{in} inlet discharged coefficient	0.4	0.8	0.4	0.4	-
Cd_{grid} grid discharged coefficient	0.5	-	0.5	0.5	-

For the simulated evaporative model, the following input values were used: l = 0.25 m, le = 1/ξ for ξ = 117.2 m^2/m^3, $A_s = A_t = 0.95$ m^2, q_{rw} = WF/As/1000×60 m^3/h for WF = 20 l/min×m^2.

The constant terms of the simulated plastic mesh pad for the thickness of 250 mm were presented in [21]. The following values were obtained: $d_2 = 4.5715$, $e_2 = -0.0210$, $f_2 = 4573.5195$, $\beta_2 = 1.6951$, m = 0.1926, n = 0.1198.

The simulation results are shown in Figure 11 and Table 3.

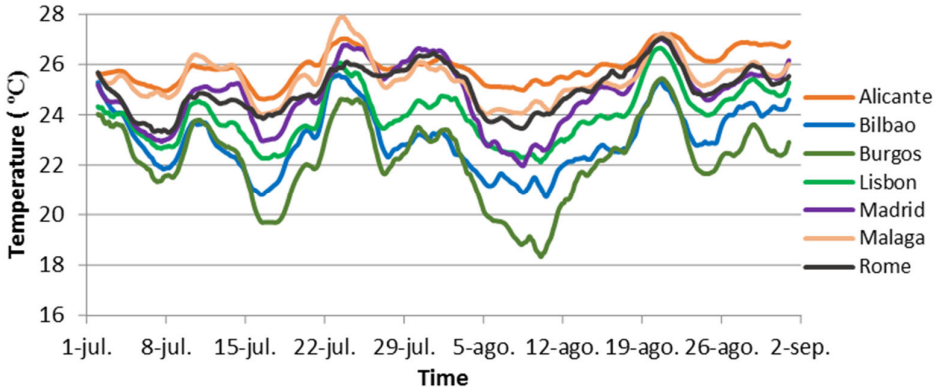

Figure 11. Average daily indoor temperature.

Table 3. Simulation results.

Location	Qv (kWh)	Airflow (m^3)	T_I max (°C)	T_I min (°C)	T_E max (°C)	T_E min (°C)	ΔT_I (ºC)	ΔT_E (°C)
Alicante	412	775,879	28.4	23.9	34.7	19	4.48	15.8
Bilbao	398	707,544	26.6	19.9	35.8	12.5	6.68	23.3
Burgos	511	658,588	26.7	16.9	36.7	7.25	9.88	29.5
Lisbon	398	684,262	27.9	20.7	37.15	15.5	7.15	21.7
Madrid	609	768,861	28.3	21.1	38.3	14.55	7.29	23.8
Málaga	429	742,782	28.8	23.2	38.7	17.55	5.62	21.1
Rome	416	712,429	28.2	22.5	33.3	15.35	5.74	18

3.3. Index Analysis

To evaluate the performance of the PDEC system, three reference indexes were proposed. Cooling energy potential, *CEP*, was the cooling energy (Q_v) per ventilated air volume (q_{tot}) in Wh/m^3, temperature cooling potential, *TCP*, was the ratio between the outdoor and indoor temperature oscillation and ventilation cooling potential, *VCP*, was the ratio between the comfort hours (h_{comf}) and the total number of hours (h_{tot}). The indoor comfort condition was set for a temperature below 26 °C.

$$CEP = \frac{Qv}{q_{tot}} \quad (11)$$

$$TCP = \frac{\Delta T_E}{\Delta T_I} \quad (12)$$

$$VCP = \frac{h_{comf}}{h_{tot}} \quad (13)$$

The *CEP* index indicated the cooling energy potential that the system was capable of providing in a specific climate; a higher value meant higher system performance. A low *TCP* value meant higher indoor temperature oscillation compared to the outdoor temperature oscillation. The *VCP* measured the percentage of comfort hours, with respect to the total hours.

The results of these indexes for each location are shown in Table 4.

Table 4. Index results.

Location	CEP (Wh/m^3)	TCP	VCP
Alicante	0.53	3.52	0.55
Bilbao	0.56	3.49	0.98
Burgos	0.78	2.98	0.99
Lisbon	0.58	3.03	0.94
Madrid	0.79	3.26	0.78
Málaga	0.58	3.75	0.72
Rome	0.58	3.13	0.80

4. Discussion

The highest ventilation flow corresponded to Alicante (hot climate with moderate humidity, $T_E > 25$ °C, 40% < RH < 65%), which presented the highest horizontal solar radiation, with 523 W/m^2, and a cooling energy provided by ventilation (Q_v) of 412 kWh for the studied period. In the case of Madrid (hot and dry climate, $T_E > 25$ °C, RH < 40%), the flow rate was slightly lower, but the system was capable of providing the highest ventilation cooling energy, up to 609 kWh. Burgos (cold climate with moderate humidity, $T_E < 21$ °C, 40% < RH < 65%) presented the lowest airflow but on the other hand, a high Q_v. The highest ratio of cooling energy per ventilated volume was found in Madrid and Burgos,

with 0.79 and 0.78 Wh/m^3, respectively. Alicante had the lowest value, with 0.53 Wh/m^3; although it had the highest ventilation flow rate, the evaporative system presented the lowest performance. The maximum hourly cooling energy demand obtained in the experimental validation of the reference building was 2.78 kW. To cover this peak demand, a Toshiba air conditioner model RAS-13 with a nominal capacity of 3.1 kW and an indoor unit flow rate of 550 m^3/h was selected to provide a cooling energy per air volume of 5.63 Wh/m^3. This result could be compared with the maximum value of 0.79 Wh/m^3 obtained for Madrid (T_E > 25 °C, RH < 40%), which accounted for 14% of this value.

The cooling temperature potential (TCP) predicted the cooling capacity of the building with respect to outdoor temperature oscillations. Burgos had the lowest value of 2.98, slightly lower than Lisbon and Rome (temperate and wet climate, 21 °C < T_E < 25 °C, RH > 65%). This indicated a higher indoor temperature oscillation (with high temperature drops) compared to the outdoor temperature oscillation. In the interpretation of this index, a low value implied oscillating indoor temperatures, while a high value implied more damped indoor temperatures.

The highest VCP value was obtained for Burgos (T_E < 21 °C, 40% < RH < 65%), with 99% comfort hours, followed by Bilbao (T_E < 21 °C, RH > 65%) and Lisbon (21 °C < T_E < 25 °C, RH > 65%), with 98% and 94%, respectively.

Analysing these three indexes in all the proposed climates, Burgos was the location where the system had the highest performance, with a high CEP value of 0.79 Wh/m^3, a low TCP value of 2.98 and a VCP close to the unit. Lisbon had a low CEP, although a high indoor temperature oscillation was obtained, reaching a minimum of 20.7 °C, as a consequence of the low temperatures during the night and a high indoor comfort ratio. Alicante, however, had the lowest performance for all the evaluated indexes. In the case of Bilbao, the evaporative system presented a high comfort ratio, although the values of CEP and TCP did not indicate high performance of the system. This was due to the fact that the average daily outdoor temperature was low and therefore, the ventilation was able to provide a large number of hours of comfort, although the performance of the evaporative system was low. In the case of Burgos and Bilbao, it would be appropriate to consider a natural ventilation system alone. As can be seen in Figure 4 above, Madrid had the highest outdoor temperatures and also a low TCP. The evaporative system had high performance, even though the comfort hours were limited in periods with high outdoor temperatures.

To analyse the effect that wind had on the total flow rate provided by the evaporative system, the cases of Burgos (U = 4 m/s, α = 5°) and Madrid (U = 2 m/s, α = 5°) were compared. The wind speed in Burgos was twice as high as in Madrid; however, the air flow supplied by the evaporative system was higher in Madrid (768,861 m^3 versus 658,588 m^3). This result was due to the lower humidity of the climate in Madrid (32.5%) compared to Burgos (53%), which resulted in a higher temperature difference. Hence, there was a stronger influence of the temperature and humidity of the local climate, with respect to the wind speed, on the flow provided by the PDEC system. Table 5 provides a classification of each climate according to the indexes analysed for the following proposed parameters: outdoor temperature, performance, comfort and applicability.

Table 5. Climate results.

Zone	Outdoor Temp.	Performance	Comfort	Applicability
Climate 1 (Madrid)	High	High	Medium	High
Climate 2 (Alicante, Málaga)	High	Medium	Medium-low	Medium
Climate 3 (Burgos)	Low	High	High	Low
Climate 4 (Bilbao)	Low	Medium	High	Low
Climate 5 (Lisbon, Rome)	Medium	Medium	Medium-high	Medium

The quality of the evaporative system to be applied in a specific climate (applicability) was determined by the qualitative evaluation of these parameters from the values of the indexes (CEP, TCP, VCP). The qualitative level of the parameter of outdoor temperature was established by the classification of the type of climate, as described in Section 3.1, where a cold climate corresponded to a low parameter, and a temperate and a hot climate corresponded to a medium and a high parameter, respectively. Regarding the level of the performance parameter, it was set from the value of the CEP index: high for CEP > 0.7 Wh/m^3, medium for 0.5 < CEP < 0.7 Wh/m^3 and low for CEP < 0.5 Wh/m^3. High comfort would correspond to a CEP value close to 1 and low comfort to a value close to 0.5.

By analysing the proposed indexes together, it was possible to evaluate and make decisions on the incorporation of PDEC systems, combined with natural ventilation solutions, in the refrigeration of residential buildings. Although the VCP index predicted the hours that the evaporative system was capable of providing comfort, the analysis of the other two indexes gave additional information on the performance of the PDEC system in a specific climate and building.

The applicability defined above was classified according to the level of the parameters of outdoor temperature, performance and comfort. The more these parameters increased from low to high, the higher the applicability. The outdoor temperature parameter was the most decisive parameter for determining the level of applicability, as can be seen in Table 5.

In the case of climate 1, the applicability was high because the outdoor temperature and performance parameter was high and the comfort parameter was medium. Climate 2, on the other hand, also had a medium outdoor temperature parameter, but the other two parameters were medium-low, which resulted in medium applicability. Climates 3 and 4 had a low outdoor temperature level; therefore, as discussed above, a ventilation strategy could be applied without the need for an evaporative system. Climate 5 presented medium parameters and hence, its applicability was medium.

5. Conclusions

The objective of this study was to evaluate the performance of an evaporative PDEC system, assisted by solar chimneys in five locations in Spain and two locations in Italy and Portugal, analysing three proposed indexes. A full-scale building energy model, developed in TRNSYS from the experimental models presented in [20,21], was used.

It was derived from [20] that the combination of thermal and airflow models using EES and TRNSYS was suitable for predicting the ventilation flow rates and indoor temperatures generated by a PDEC system. In this simulation study, the influence of the building geometry on the airflow field was addressed, using the correlation of Equation 7 [24].The locations analysed were classified into 5 different climate types. The simulated system produced specific results for the indoor conditions in each case.

The cooling energy potential (CEP) ranged between 0.53 Wh/m^3 and 0.79 Wh/m^3 for Alicante (climate 2) and Madrid (climate 1), respectively. The highest performance and applicability was obtained for Madrid (climate 1), where a value for the ventilation cooling potential (VCP) of 78% was obtained. Burgos (climate 3) and Bilbao (climate 4) presented VCP values of 99% and 98% respectively, although the applicability of the evaporative system was low. In both cases, due to the low outdoor temperature, a natural ventilation strategy, with intermittent supply of the evaporative system, would be appropriate. Malaga presented good results, with oscillating outdoor temperatures, damped indoor temperatures and a comfort ratio of 72%.

The study shows the importance of outdoor temperature and humidity conditions on the performance and applicability of evaporative systems beyond the ventilation flow rates provided by the system and the influence of wind. In addition, the flow rate provided by the cooling system was also influenced to a large extent by the flow rate extracted at the solar chimneys.

A PDEC system, assisted by solar chimneys, can provide interesting energy savings in fulfilment of the objectives set by the EU. The regulations do not establish a recommendation or obligation for the use of these systems in certain climates. The study undertaken presents certain criteria for evaluating an evaporative system in a specific climate in order to analyse its performance and applicability in the project phase.

An experimental study of the direct evaporative pad combined with the natural ventilation of the reference building could be studied in future projects.

Author Contributions: Conceptualization, Methodology, Software, Validation, Formal Analysis, Investigation, Resources, Writing—Original Draft, Writing—Review & Editing, Visualization, A.S.; Validation, Investigation, Resources, Supervision, Writing—Review & Editing, P.M.; Supervision, Writing—Review & Editing, V.M.S.; Conceptualization, Methodology, Validation, Formal Analysis, Writing—Review & Editing, Investigation, Resources, Supervision, P.J.M. All authors have read and agreed to the published version of the manuscript.

Funding: This research was funded by FEDER/Ministerio de Ciencia e Innovación Agencia Estatal de Investigación through Spanish research projects ENE2017-83729-C3-1-R and ENE2017-83729-C3-3-R, supported by FEDER funds.

Institutional Review Board Statement: Not applicable.

Informed Consent Statement: Not applicable.

Data Availability Statement: All data are specified in the article.

Conflicts of Interest: The authors declare no conflict of interest.

Nomenclature

A	area (m^2)
A_s	total exposed surface area of the pad module (m^2)
B	building breadth (m)
Cd	discharge coefficient
Cp	pressure coefficient
CEP	cooling energy potential (kWh/m^3)
D	building depth (m)
g	gravitational force per unit mass (m/s^2)
h_{comf}	hours in comfort (h)
h_{tot}	total hours (h)
H	room height (m)
HVAC	heating, ventilation and air conditioning
l	thickness of the evaporative pad (m)
le	characteristic dimension of the pad module, le = 1/ξ (m)
L	chimney height (m)
M	sign flow direction
q	air flow rate (m^3/s)
Qv	ventilation cooling energy (kWh)
q_{rw}	volumetric flow rate of recirculated water (m^3/s)
S	building depth to breadth side ratio
T	temperature (°C)
TCP	temperature cooling potential
U	wind speed (m/s)
v	air velocity (m/s)
VCP	ventilation cooling potential
WF	water flow rate per exposed pad surface area (l/min m^2)
z	height of opening above ground level (m)

Greek Symbols

α	wind angle from normal to side (°)
Δp	pressure difference (Pa)
$\Delta \varrho_0$	air density difference at ground level (kg/m^3)
ΔT	temperature difference (K)
ξ	compactness of the evaporative pad (m^2/m^3)
η	saturation efficiency
ϱ	air density (kg/m^3)

Subscripts

c	chimney
eff	effective
eva	evaporative
E	outdoor
grid	grid
in	inlet
I	indoor
out	outlet
t	window tower
wb	wet bulb

References

1. Monghasemi, N.; Vadiee, A. A review of solar chimney integrated systems for space heating and cooling application. *Renew. Sustain. Energy Rev.* **2017**, *81*, 2714–2730, doi:10.1016/j.rser.2017.06.078.
2. Saleem, A.A.; Bady, M.; Ookawara, S.; Abdel-Rahman, A.K. Achieving standard natural ventilation rate of dwellings in a hot-arid climate using solar chimney. *Energy Build.* **2016**, *133*, 360–370, doi:10.1016/j.enbuild.2016.10.001.
3. Kang, D.; Strand, R.K. Analysis of the system response of a spray passive downdraft evaporative cooling system. *Build. Environ.* **2019**, *157*, 101–111, doi:10.1016/j.buildenv.2019.04.037.
4. Cuce, P.M.; Riffat, S. A state of the art review of evaporative cooling systems for building applications. *Renew. Sustain. Energy Rev.* **2016**, *54*, 1240–1249, doi:10.1016/j.rser.2015.10.066.
5. Ahmed, T.; Kumar, P.; Mottet, L. Natural ventilation in warm climates: The challenges of thermal comfort, heatwave resilience and indoor air quality. *Renew. Sustain. Energy Rev.* **2021**, *138*, 110669, doi:10.1016/j.rser.2020.110669.
6. Rong, L.; Pedersen, P.; Jensen, T.L.; Morsing, S.; Zhang, G. Dynamic performance of an evaporative cooling pad investigated in a wind tunnel for application in hot and arid climate. *Biosyst. Eng.* **2017**, *156*, 173–182, doi:10.1016/j.biosystemseng.2017.02.003.
7. Kovačević, I.; Sourbron, M. The numerical model for direct evaporative cooler. *Appl. Therm. Eng.* **2017**, *113*, 8–19, doi:10.1016/j.applthermaleng.2016.11.025.
8. Sohani, A.; Sayyaadi, H. Design and retrofit optimization of the cellulose evaporative cooling pad systems at diverse climatic conditions. *Appl. Therm. Eng.* **2017**, *123*, 1396–1418, doi:10.1016/j.applthermaleng.2017.05.120.
9. Nada, S.A.; Fouda, A.; Mahmoud, M.A.; Elattar, H.F. Experimental investigation of energy and exergy performance of a direct evaporative cooler using a new pad type. *Energy Build.* **2019**, *203*, doi:10.1016/j.enbuild.2019.109449.
10. Doğramacı, P.A.; Aydın, D. Comparative experimental investigation of novel organic materials for direct evaporative cooling applications in hot-dry climate. *J. Build. Eng.* **2020**, *30*, doi:10.1016/j.jobe.2020.101240.
11. Laknizi, A.; Mahdaoui, M.; Abdellah, A.B.; Anoune, K.; Bakhouya, M.; Ezbakhe, H. Performance analysis and optimal parameters of a direct evaporative pad cooling system under the climate conditions of Morocco. *Case Stud. Therm. Eng.* **2019**, *13*, 100362, doi:10.1016/j.csite.2018.11.013.
12. Naderi, E.; Sajadi, B.; Naderi, E.; Bakhti, B. Simulation-based performance analysis of residential direct evaporative coolers in four climate regions of Iran. *J. Build. Eng.* **2020**, *32*, 101514, doi:10.1016/j.jobe.2020.101514.
13. Yang, Y.; Cui, G.; Lan, C.Q. Developments in evaporative cooling and enhanced evaporative cooling—A review. *Renew. Sustain. Energy Rev.* **2019**, *113*, 109230, doi:10.1016/j.rser.2019.06.037.
14. Yan, M.; He, S.; Li, N.; Huang, X.; Gao, M.; Xu, M.; Miao, J.; Lu, Y.; Hooman, K.; Che, J.; et al. Experimental investigation on a novel arrangement of wet medium for evaporative cooling of air. *Int. J. Refrig.* **2021**, *124*, 64–74, doi:10.1016/j.ijrefrig.2020.12.014.
15. Aparicio-Ruiz, P.; Schiano-Phan, R.; Salmerón-Lissén, J.M. Climatic applicability of downdraught evaporative cooling in the United States of America. *Build. Environ.* **2018**, *136*, 162–176, doi:10.1016/j.buildenv.2018.03.039.
16. Campaniço, H.; Soares, P.M.M.; Hollmuller, P.; Cardoso, R.M. Climatic cooling potential and building cooling demand savings: High resolution spatiotemporal analysis of direct ventilation and evaporative cooling for the Iberian Peninsula. *Renew. Energy* **2016**, *85*, 766–776, doi:10.1016/j.renene.2015.07.038.

17. Campaniço, H.; Soares, P.M.M.; Cardoso, R.M.; Hollmuller, P. Impact of climate change on building cooling potential of direct ventilation and evaporative cooling: A high resolution view for the Iberian Peninsula. *Energy Build.* **2019**, *192*, 31–44, doi:10.1016/j.enbuild.2019.03.017.
18. Kang, D.; Strand, R.K. Significance of parameters affecting the performance of a passive down-draft evaporative cooling (PDEC) tower with a spray system. *Appl. Energy* **2016**, *178*, 269–280, doi:10.1016/j.apenergy.2016.06.055.
19. Kang, D.; Strand, R.K. Modeling of simultaneous heat and mass transfer within passive down-draft evaporative cooling (PDEC) towers with spray in FLUENT. *Energy Build.* **2013**, doi:10.1016/j.enbuild.2013.02.039.
20. Soto, A.; Martínez, P.J.; Martínez, P.; Tudela, J.A. Simulation and experimental study of residential building with north side wind tower assisted by solar chimneys. *J. Build. Eng.* **2021**, *43*, 102562, doi:10.1016/j.jobe.2021.102562.
21. Martínez, P.; Ruiz, J.; Martínez, P.J.; Kaiser, A.S.; Lucas, M. Experimental study of the energy and exergy performance of a plastic mesh evaporative pad used in air conditioning applications. *Appl. Therm. Eng.* **2018**, *138*, 675–685, doi:10.1016/j.applthermaleng.2018.04.065.
22. Aschaber, J.; Hiller, M.; Weber, R. Trnsys17: New features of the multizone building model. In Proceedings of the IBPSA 2009-International Building Performance Simulation Association Conference, Glasgow, Scotland, 27–30 July 2009.
23. Klein, S.; Nellis, G. *Engineering Equation Solver (EES) for Microsoft Windows Operating Systems, Professional Versions*; F-Chart SoftwarE: Madison, WI, USA, 2014.
24. Muehleisen, R.T.; Patrizi, S. A new parametric equation for the wind pressure coefficient for low-rise buildings. *Energy Build.* **2013**, *57*, 245–249, doi:10.1016/j.enbuild.2012.10.051.
25. Meteonorm. Meteonorm-Global Meteorological Database. 2012. Available online: http://meteonorm.com/ (accessed on March 26, 2021).